JOURNAL OF SPACECRAFT AND ROCKETS
Vol. 40, No. 2, March–April 2003

Assessment of Thermovibrational Theory: Application to *G*-Jitter on the Space Station

R. Savino* and M. Lappa†
University of Naples, "Federico II," 80125 Naples, Italy

The numerical modeling of the effects of *g*-jitter (oscillatory residual acceleration disturbances) on fluid dynamics experiments onboard the International Space Station is discussed. The aim is an assessment of the thermovibrational theory, based on the time-averaging technique and the evaluation of the orders of magnitude of all of the terms appearing in the complete equations, identifying the role and the importance of average and oscillatory terms. The identification of the most important terms in the momentum and in the energy equation is made by an a posteriori order of magnitude analysis by means of the numerical solution of the unsteady full Navier–Stokes equations. Different flow regimes are identified, and some apparent contradictions in the current literature on the effects of *g*-jitter are clarified. The set of reduced equations and the associated range of validity is of great potential interest for the scientific community to develop analytical and/or mixed numerical/analytical solutions that can lead to a significant reduction of the often prohibitive computational time required for the simulation of the complex phenomena under investigation.

Nomenclature

b = displacement amplitude, m
c = mass concentration
f = frequency, 1/s
$\boldsymbol{g}_\omega$ = maximum acceleration, m/s^2
$\boldsymbol{g}_0$ = Earth gravity acceleration, 9.81 m/s^2
L = size of the cell, m
$\boldsymbol{n}$ = unit vector in the acceleration direction
Pr = Prandtl number (ν/α)
p = pressure, Pa
Ra_v = vibrational Rayleigh number
$\boldsymbol{r}$ = position vector, m
T = temperature, K
t = time, s
u = velocity component along x, m/s
$\boldsymbol{V}$ = velocity vector, m/s
v = velocity component along y, m/s
α = thermal diffusivity, m^2/s
β_T = thermal expansion coefficient, 1/K
ΔT = characteristic temperature difference imposed across the cell, K
ΔT_j = local amplitude of the temperature oscillation, K
Δt = time step, s
δT = temperature disturbance, K
$\bar{\varepsilon}_T$ = dimensionless measure of the overall time-average disturbance
ε'_T = dimensionless measure of the overall oscillatory disturbance
Λ = dimensionless displacement, $b(\beta_T \Delta T/L)$
ν = kinematic viscosity, m^2/s
ρ = density, kg/m^3
Φ'_i = ratios between the oscillatory term i and the leading term in the momentum (subscript v) and energy (subscript T) equations
$\overline{\Phi_i}$ = ratios between the time averaged term i and the leading term in the momentum (subscript v) and energy (subscript T) equations
Ω = dimensionless angular frequency, $(\omega L^2/\alpha)$
ω = angular frequency, 1/s
∇ = nabla operator, 1/m
∇^2 = Laplace operator, 1/m^2

Subscripts

c = cold side
d = diffusive conditions
h = hot side
j = grid point j of the mesh
max = maximum value
min = minimum value
0 = reference conditions

Introduction

EXPLOITATION of microgravity environments in physical sciences (fluid science, material science) is motivated in most cases by the establishment of purely diffusive regimes, that is, processes that take place in quiescent fluid media, that would prevail in an ideal (0-g) environment. Typical experiments that would benefit from a quiescent or a quasi-quiescent condition are crystal growth, solidification processes, experiments for the measurement of diffusion or thermodiffusion coefficients, and many others. These experiments are characterized by heat and mass transfer processes in fluid phases in the presence of density gradients, caused by thermal gradients (due to heat exchange or to latent heat release during a phase change) or by the concentration of gradients arising, for example, from the rejection or the incorporation of solute at a solidification interface.

In the presence of accelerations (including steady and periodic accelerations of different amplitudes and frequencies), the velocity, temperature, and concentration fields can be determined by the differential balance equations (for mass, momentum, energy, and mass species). These accelerations typically induce convective motions that may be important for fluid and material science microgravity experimentation on the International Space Station (ISS), even if the residual gravity is reduced by several orders of magnitude and relatively small amplitude g-jitter is present (Fig. 1).

Oscillatory g-jitter includes all of the periodic time-dependent accelerations that can be approximated by sinusoidal functions. The most common sources of these accelerations are structural vibrations, for example, at the fundamental natural frequencies,

Received 30 October 2001; revision received 5 August 2002; accepted for publication 16 September 2002.

*Associate Professor of Fluid Dynamics, Department of Space Science and Engineering, P. le Tecchio 80; rasavino@unina.it.

†Ph.D. Student, Aerospace Engineer, Department of Space Science and Engineering, P. le Tecchio 80; marlappa@marscenter.it.

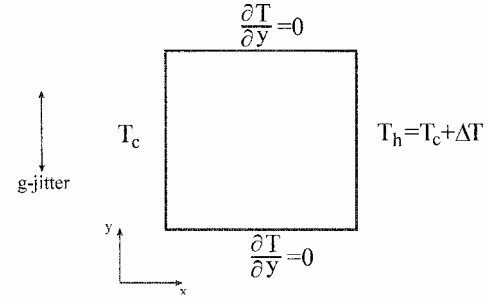

Fig. 1a Study case: two-dimensional cell, single fluid with high Prandtl numbers at periodic conditions.

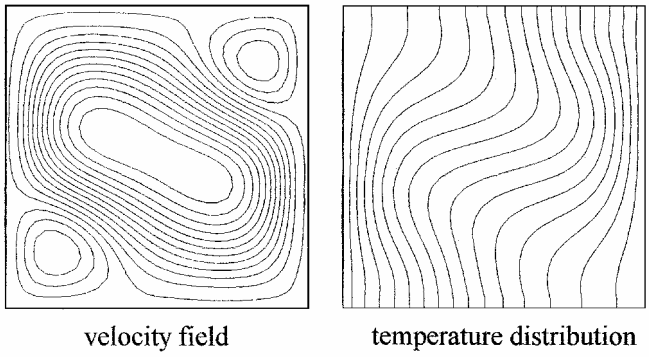

Fig. 1b Typical flow organization: streamlines and isotherms related to the average flow; Ra_v = 33,000 and Pr = 15.

equipment operations, and crew activity, for example, repetitive exercises that induce cyclic displacement of the position of the test cell.

The behavior of fluid systems subject to sinusoidal accelerations has been the subject of intensive research in the last decade. Many theoretical and numerical studies have been dedicated to this topic.[1–6]

It has been shown by an extensive numerical experimentation[7–11] that, when soliciting the fluid cell by periodic accelerations, the diffusive temperature distribution $T_d(\boldsymbol{r}, t)$ and/or the concentration distribution $c_d(\boldsymbol{r}, t)$ are distorted and the difference (suitably defined) between the temperature (and/or concentration) distribution and the diffusive (ideal) one can define the g-jitter "disturbance." (If this disturbance exceeds some threshold values, one may say that the microgravity environment of the platform is not "tolerable" by the experiment.) In particular, a number of computations for different study cases pointed out that the velocity field $\boldsymbol{V}$, induced by periodic $\boldsymbol{g}$ is made up by an average value $\bar{\boldsymbol{V}}$ plus a periodic oscillation of amplitude $\boldsymbol{V}'$ ($\boldsymbol{V} = \bar{\boldsymbol{V}} + \boldsymbol{V}'$) at the g-jitter frequency f or at frequencies multiple of f. As a result of the convective field, the scalar quantities (temperature and/or species concentration) are also distorted. These distortions are also made up by a steady addition an oscillatory contribution.

Theoretical[1,4,6,7] and numerical results[3,10,12] available in the literature pointed out that different situations may occur, depending on the oscillation frequency. Numerical results by Savino and Monti[12] show that, when frequency is increased, there is a first regime characterized by relatively large oscillatory velocity and oscillatory temperature disturbances and relatively small time-average steady disturbances. At high frequencies, the oscillatory thermal disturbances are very small with respect to the steady ones induced by the time-average part of the velocity field (Fig. 2a, to be discussed later). This behavior suggested that introduce strong simplifications be introduced in the analysis of the disturbances computation. In particular, according to the Gershuni et al. formulation[13] the time-averaged distortions can be simply computed, that is, with much less computation time, by a simplified set of equations in terms of quantities averaged over the oscillation period.

The present work is intended to extend the averaging technique (initially introduced by the thermovibrational theory) that is valid only at the extreme values of small amplitudes of the periodic displacements and high frequencies. The extension is obtained by evaluating the order of magnitude of all of the terms appearing in the complete equations and by identifying the role and the importance of the average and the periodic terms. Even though the results strictly refer to the specific study case (two-dimensional cell, single fluid with high Prandtl numbers at periodic conditions; Fig. 1), a number of conclusions can apply to more general cases, as will be seen in the following sections of the paper.

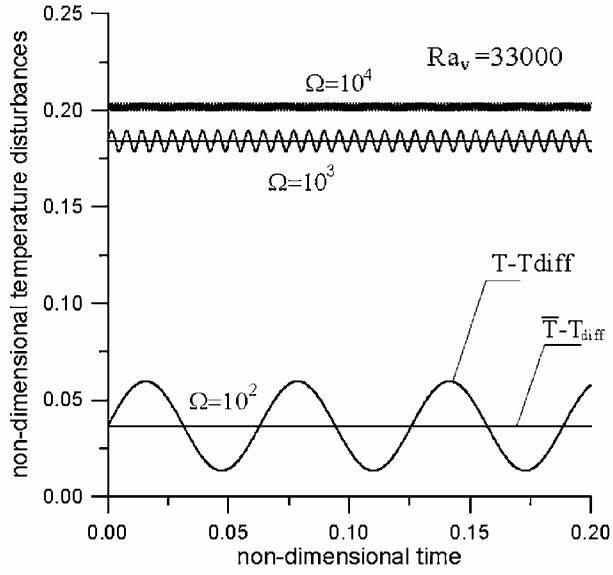

Fig. 2a Nondimensional temperature at $x = 0.25, y = 0.5$ ($\Omega = \omega L^2/\alpha$).

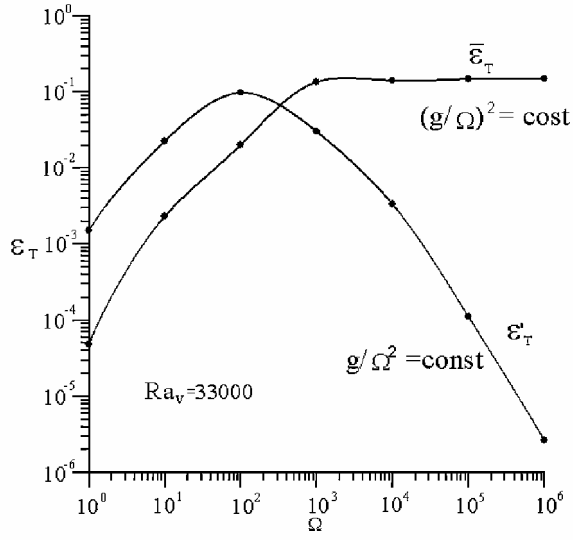

Fig. 2b Disturbances vs Ω, where $\Omega = \omega L^2/\alpha$.

The identification of the most important terms in the momentum and in the energy equation will be made with the help of the numerical solution of the unsteady full Navier–Stokes equations and will help in identifying a simplified set of equations (by dropping a number of terms of smaller orders of magnitude) and their range of validity. The proposed methodology is a sort of a posteriori order of magnitude analysis (OMA) that refers to both the full and average Navier–Stokes and energy equations, of all of the terms of the equations. Each variable (T, $\boldsymbol{V}$, p) has been decomposed in the average and oscillatory contribution. The splitting of the variables allows a very detailed OMA that is able to explain the numerical results obtained by different authors.

As mentioned, for the given experimental conditions there is a strong dependence of both types of disturbances (average and periodic) on the g-jitter frequency. Amplitudes of the periodic temperature disturbances tend quickly to decrease with frequency; conversely, the average disturbances are less dependent on the frequency so that one expects the unsteady disturbances to "prevail" over the steady ones at low frequencies (and vice versa).

The aim of the present paper is the separation of the steady oscillations from the periodic oscillations at the level of the Navier–Stokes equations, to single out which terms are responsible for the generation of velocity and temperature distribution. In particular, we want to 1) generalize the separation between oscillatory and time-average difference between the complete solution and the purely diffusive steady state process, T_d; 2) identify the leading terms in the equations; and 3) evaluate the relative importance of each term as function of the frequency.

The identification of a set of reduced equations and associated ranges of validity is of great potential importance for the scientific community. A simplified set of equations in fact can be used to obtain analytical or numerical solutions of the problem. Generally, the methods attempted by the different researchers to yield these simplified solutions fall into two categories: 1) some set of alternative equations by mathematical transformation and manipulation of the original set (e.g., Gershuni and Lyubimov[14]) and 2) asymptotic series expansions and analytical/numerical solutions.[15] In both cases the probability of success are largely improved by the simplification (by dropping some terms) of the initial set of nonlinear equations. By these techniques, the solution algorithm can be accelerated up to 100 times with respect to the case of the solution of the complete Navier–Stokes equations.

The introduction of these techniques however is out of the scope of the present work. Here the analysis is restricted to make available simplified a set of equations to the scientific community.

Definition of Disturbances

Let us consider disturbances induced in a fluid cell by a sinusoidal displacement

$$\boldsymbol{s}(t) = b \sin \omega t \, \boldsymbol{n} \tag{1}$$

that induces an acceleration

$$\boldsymbol{g}(t) = \boldsymbol{g}_\omega \sin \omega t \tag{2}$$

where $\boldsymbol{g}_\omega = b\omega^2 \boldsymbol{n}$. As in most cases in microgravity experimentation, we take the reference conditions to be those prevailing in an ideal 0-g environment that, for most of the experiments, imply quiescent conditions ($\boldsymbol{V} = \boldsymbol{0}$) with mass and energy transported only by diffusion. In the following, subscript d is used for the parameters corresponding to the purely diffusive conditions, for example, the temperature $T_d\,(x, y, z, t)$. The thermal disturbances induced by any acceleration will, therefore, be defined at each point (x, y, z) and at any time t as

$$\delta T = T(x, y, z, t) - T_d(x, y, z, t) \tag{3}$$

In the case of numerical integration at the grid point j of the mesh,

$$\delta T_j(t) = T_j(t) - T_{jd}(t) \tag{4}$$

The local temperature can be split into a time-averaged steady contribution plus an oscillating part ($T_j = \bar{T}_j + T'_j$) so that the local temperature disturbance is

$$\delta T_j = T_j - T_{jd} = (\bar{T}_j - T_{jd}) + T'_j \tag{5}$$

where $\bar{T}_j$ is the nondimensional local temperature averaged over the period $2\pi/\omega$ and T'_j is the oscillatory part expressed in terms of the local amplitude of the temperature oscillation (ΔT_j):

$$T'_j = \Delta T_j f_j(\omega) \tag{6}$$

where $f_j(\omega)$ is a periodic, zero time-average function, (for example, $f_j(\omega) = \sin(\omega t + \varphi_j)$. In general $\bar{T}_j$ and ΔT_j are function of time until periodic conditions are reached. We will refer to disturbances prevailing in the periodic regime ($t \to \infty$) after an initial transient.

Two different overall thermal disturbance parameters (over all of the grid points N) can be defined:

$$\bar{\varepsilon}_T = \frac{1}{N} \sum_{j=1}^{N} \left| \frac{(\overline{T_j} - T_{jd})}{\Delta T} \right| \tag{7a}$$

$$\varepsilon'_T = \frac{1}{N} \sum_{j=1}^{N} \left| \frac{(\Delta T_j)}{\Delta T} \right| \tag{7b}$$

where ΔT is the characteristic temperature difference imposed across the cell (Fig. 1a). The two disturbances parameters are both constant with time at periodic conditions. If both $\bar{\varepsilon}_T$ and ε'_T are $\ll 1$, one can assume that the purely diffusive regime is not disturbed by the presence of the onboard acceleration $\boldsymbol{g}(t)$.

One can rightly suspect that the two disturbance parameters may play a different role in different processes, for example, crystal growth, solidification processes, sedimentation, and that no comparison can be made between the two types of disturbances; the order of magnitude of $\bar{\varepsilon}_T$ and ε'_T for the negligibility of the thermal disturbances may be different. This difference is a further reason to evaluate separately the amplitude of the periodic disturbances (in velocity and temperature) related to the angular velocity ω of the forcing g-jitter and the steady disturbance (again in velocity and temperature) that results from the streaming motion due to the nonlinear convective terms in the equation.

The analysis that follows will clarify a number of apparent contradictions encountered in the literature on the estimate of the dependence of the temperature (and/or concentration) disturbances on the g-jitter frequency. In fact, the results that the disturbances depend on acceleration and frequency as g_ω^2/ω^2 (Monti and Savino[9]) or as g_ω/ω^2 (Monti et al.[1]) are both correct, but refer to the two types of disturbances: The first refers to $\bar{\varepsilon}_T$ and the second to ε'_T as shown in Fig. 2b. The different conclusions of the two analyses depend on the different a priori assumptions made in the momentum and energy equations.

In Ref. 1, all of the nonlinear terms were neglected for high values of the frequency. In the Gershuni treatment (as it will be shown later) the nonlinear, nonzero time-average terms that are negligible in the momentum and energy equations are taken into account in the time-average equations to find the time-average velocity and temperature distributions.

Reference Case

A two-dimensional test cell with square section of side L in the plane xy is filled with a homogeneous Newtonian liquid (silicone oil with kinematic viscosity $\nu = 1$cS). All of the boundaries of the cavity are solid walls (Fig. 1a). The walls at $x = 0$ and L are maintained at constant temperatures T_c and $T_h = T_c + \Delta T$; the other boundaries are adiabatic. A simple, periodic, sinusoidal acceleration is applied [defined by Eqs. (1) and (2)], characterized by the magnitude g_ω and the direction $\boldsymbol{n}$ perpendicular to the imposed temperature gradient.

For the chosen configuration ($\Delta T = 60$ K and cell size 5×5 cm^2) and liquid with Prandtl number $Pr = 15$ ($\alpha = 6.6 \times 10^{-4}$ cm^2/s and $\beta_T = 1.3 \times 10^{-3}$ 1/K), the typical flow organization is that shown in Fig. 1b by the streamlines and the isotherms related to the average flow. A periodic oscillating temperature and velocity field is superimposed on the average field after a sufficient time has elapsed during which constant boundary conditions are maintained.

The relative importance of the temperature periodic oscillations with respect to the steady disturbances ($\bar{T} - T_d$) can be seen in Fig. 2a, where the nondimensional temperature disturbances at a typical field point are reported at different acceleration frequencies. The examples shown refer to three different frequencies proportional to their amplitudes ($g_\omega/\omega = b\omega = \text{const}$). Independent of the magnitude of the steady and pulsating disturbances, Fig. 2a intend to show that, for increasing frequencies ($\Omega = \omega L^2/\alpha$), the oscillating part becomes much smaller than the steady part, as will be discussed in detail later.

Numerical Solution Technique

The flow is governed by the continuity, Navier–Stokes, and energy equations that in dimensional conservative form read

$$\nabla \cdot \boldsymbol{V} = 0 \tag{8a}$$

$$\frac{\partial \boldsymbol{V}}{\partial t} = -\frac{1}{\rho_0} \nabla p - \nabla \cdot [\boldsymbol{V}\boldsymbol{V}] + \nu \nabla^2 \boldsymbol{V} - b\omega^2 \beta_T \sin(\omega t)(T - T_0)\boldsymbol{n} \tag{8b}$$

$$\frac{\partial T}{\partial t} = -\nabla \cdot [\boldsymbol{V}T] + \alpha \nabla^2 T \tag{8c}$$

where ρ_0 and T_0 relate to reference conditions, for example, temperature of the cold wall, and β_T is the (constant) thermal expansion coefficient $\beta_T = (1/\rho)(\partial\rho/\partial T)$.

From now on, we use nondimensional quantities; we denote nondimensional T, $\boldsymbol{V}$, and p by the same symbols used in Eqs. (8). Equations (8), in nondimensional form, read

$$\nabla \cdot \boldsymbol{V} = 0 \tag{9a}$$

$$\frac{\partial \boldsymbol{V}}{\partial t} = -\nabla p - \nabla \cdot [\boldsymbol{V}\boldsymbol{V}] + Pr\nabla^2 \boldsymbol{V} - \frac{\Lambda\Omega^2}{Pr}\sin(\Omega t) T \boldsymbol{n} \tag{9b}$$

$$\frac{\partial T}{\partial t} = -\nabla \cdot [\boldsymbol{V}T] + \nabla^2 T \tag{9c}$$

The nondimensional form results from scaling the coordinates by a characteristic length of the problem under investigation, L, and the velocity components u and v by the energy diffusion velocity $V_\alpha = \alpha/L$. The scales for the time and the pressure are, respectively, L^2/α and $\rho_0(V_\alpha)^2 = \rho_0\alpha^2/L^2$. The temperature, measured with respect to the reference temperature T_0, for example, the cold wall temperature, is scaled by ΔT. The nondimensional frequency Ω and displacement Λ are defined by

$$\Omega = \omega L^2/\alpha, \qquad \Lambda = b(\beta_T \Delta T/L) \tag{10}$$

At the initial time, the liquid filling the cell is supposed to be quiescent and at a temperature corresponding to the purely diffusive situation:

$$t = 0: \qquad \boldsymbol{V}(x, y) = 0, \qquad T_d(x, y) = x \tag{11}$$

The boundary conditions on the heated walls are the no-slip condition and the temperature conditions.

On the cold wall:

$$\boldsymbol{V}(x = 0, y, t) = 0, \qquad T(x = 0, y, t) = 0 \tag{12a}$$

On the hot wall:

$$\boldsymbol{V}(x = 1, y, t) = 0, \qquad T(x = 1, y, t) = 1 \tag{12b}$$

Equations (9a–9c) subjected to the initial and boundary [Eqs. (11) and (12)] conditions were solved numerically in primitive variables by a finite difference method. The domain was discretized with a uniform mesh, and the flowfield variables were defined over a staggered grid. Forward differences in time and central-differencing schemes in space (second-order accurate) were used to discretize the partial differential equations, obtaining

$$\boldsymbol{V}^{n+1} = \boldsymbol{V}^n + \Delta t[-\nabla \cdot (\boldsymbol{V}\boldsymbol{V}) + Pr\nabla^2 \boldsymbol{V} - (\Lambda\Omega^2/Pr)\sin(\Omega t) T \boldsymbol{n}]^n - \Delta t \nabla p^n \tag{13}$$

$$T^{n+1} = T^n + \Delta t[-\nabla \cdot (\boldsymbol{V}T) + \nabla^2 T]^n \tag{14}$$

The computation of the velocity field at each time step has been split into two substeps. In the first, an approximate velocity field $\boldsymbol{V}^*$ corresponding to the correct vorticity of the field, but with $\nabla \cdot \boldsymbol{V}^* \neq 0$, is computed at time $(n + 1)$ neglecting the pressure gradient in the momentum equation, that is,

$$\boldsymbol{V}^* = \boldsymbol{V}^n + \Delta t[-\nabla \cdot (\boldsymbol{V}\boldsymbol{V}) + Pr\,\nabla^2 \boldsymbol{V} - (\Lambda\Omega^2/Pr)\sin(\Omega t) T \boldsymbol{n}]^n \tag{15}$$

In the second substep, the pressure field is computed by solving a Poisson equation resulting from the divergence of the momentum equation with the help of the continuity equation:

$$\nabla^2 p^n = (1/\Delta t)\nabla \cdot \boldsymbol{V}^* \tag{16}$$

Finally, the velocity field is updated using the computed pressure field to account for continuity:

$$\boldsymbol{V}^{n+1} = \boldsymbol{V}^* - \Delta t \nabla p^n \tag{17}$$

The Poisson equation is solved with a successive overrelaxation iterative method. The temperature field at time $(n + 1)$ is obtained from Eq. (14) after the calculation of the velocity.

Grid Refinement Study and Code Validation

The numerical model has been validated by quantitative comparisons with available numerical results. In particular, to check that the code is able to capture correctly the effect of periodic acceleration disturbances on the thermofluid-dynamic field, the results obtained solving the complete set of nonlinear and time-dependent Navier–Stokes equations (underlying the present numerical algorithm) have been compared with those obtained by Gershuni and Lyubimov[14] using their modified set of equations (valid at high frequencies and small amplitude of the disturbance residual acceleration).

A case lying in the range of applicability of the Gershuni and Lyubimov[14] formulation has been considered for comparison because 1) the simplified set of averaged equations and associated numerical results represent a robust and reliable example for comparison and 2) the simulation of the effect of high frequencies and small amplitude of the acceleration is expected to be the most weighty situation for a code dealing with the numerical solution of the complete equations; in this case, in fact, because of the intrinsic nature of the phenomena (very small oscillation period and amplitude of the disturbance), the numerical prediction of the physics is very delicate, and the numerical algorithm has to demonstrate high sensitivity and great accuracy.

The comparison has shown that the present results compose very well with those of Gershuni and Lyubimov.[14] (The simulations agree within 1%.) For the sake of brevity, the comparison is not shown in detail. For further details see previous work,[12] where the same validation was carried out and was extensively described.

In this subsection, moreover, to show the numerical convergence of the present algorithm a grid refinement study is discussed. The computations have been performed for uniform grids $Nx \times Ny$. (The first number denotes the number of collocation points in the x direction, and the second defines the grid size in the y direction.)

Grid convergence has been obtained for a resolution of 30×30 points. However, a grid 40×40 has been used for the simulations to achieve very high accuracy of the solution. The simulations typically require about 48 h of computations on a Digital 433 workstation. Note that the same results can be obtained solving the simplified set of averaged equations, in the case of high frequency g-jitter, in less than 1 h on the same computer.

Averaging Technique and Extension of the Analysis

Until now, two methods for g-jitter analysis have been considered in literature: 1) numerical computation of the full nonlinear and time-dependent Navier–Stokes equations with a time-dependent body force that gives rise to a time-dependent flow and 2) numerical solutions of the time-averaged field equations (Gershuni formulation) for the thermovibrational convection problem, obtained under the assumption of sufficiently small amplitudes ($\Lambda \ll 1$) and sufficiently large frequencies ($\Omega \gg 1$) of the g-jitter. At these conditions Gershuni and Lyubimov[14] show that, for given Prandtl number, the steady (streaming) convection depends only on one relevant dimensionless parameter, the vibrational Rayleigh number:

$$Ra_v = \frac{(b\omega\beta_T \Delta T L)^2}{2\nu\alpha} = \frac{(\beta_T \Delta T L)^2}{2\nu\alpha}\left(\frac{g_\omega}{\omega}\right)^2 = \frac{\Omega^2\Lambda^2}{2Pr} \tag{18}$$

Let us rewrite the Eqs. (9) in terms of the average values $\bar{\boldsymbol{V}}$ and $\bar{T}$ plus periodic oscillations, ($\boldsymbol{V}'$ and T': $\boldsymbol{V} = \bar{\boldsymbol{V}} + \boldsymbol{V}'$ and $T = \bar{T} + T'$. As a result of this assumption, Eqs. (9) can be written as

$$\nabla \cdot \bar{\boldsymbol{V}} + \nabla \cdot \boldsymbol{V}' = 0 \tag{19a}$$

$$\frac{\partial \bar{\boldsymbol{V}}}{\partial t} + \frac{\partial \boldsymbol{V}'}{\partial t} + (\nabla \bar{p} + \nabla p') + \nabla \cdot [\overline{\boldsymbol{V}\boldsymbol{V}}] + \nabla \cdot [\bar{\boldsymbol{V}}\boldsymbol{V}'] + \nabla \cdot [\boldsymbol{V}'\bar{\boldsymbol{V}}] + \nabla \cdot [\boldsymbol{V}'\boldsymbol{V}'] = Pr(\nabla^2 \bar{\boldsymbol{V}} + \nabla^2 \boldsymbol{V}') - \frac{\Lambda\Omega^2}{Pr}\sin(\Omega t)\bar{T}\boldsymbol{n} - \frac{\Lambda\Omega^2}{Pr}T'\sin(\Omega t)\boldsymbol{n} \tag{19b}$$

$$\frac{\partial \bar{T}}{\partial t} + \frac{\partial T'}{\partial t} + \nabla \cdot [\bar{\boldsymbol{V}}\bar{T}] + \nabla \cdot [\bar{\boldsymbol{V}}T'] + \nabla \cdot [\boldsymbol{V}'\bar{T}] + \nabla \cdot [\boldsymbol{V}'T'] = \nabla^2 \bar{T} + \nabla^2 T' \tag{19c}$$

If the values of $\boldsymbol{V}(t)$ and $T(t)$ are known at a given field point, the average values for $\boldsymbol{V}$ and T can be computed by

$$\bar{\boldsymbol{V}} = \frac{\omega}{2\pi}\int_0^{2\pi/\omega} \boldsymbol{V}\,\mathrm{d}t, \qquad \bar{T} = \frac{\omega}{2\pi}\int_0^{2\pi/\omega} T\,\mathrm{d}t \tag{20}$$

The time-dependent parts $\underline{V'}$ and T' at each instant of time can, therefore, be defined as

$$\boldsymbol{V}' = \boldsymbol{V} - \bar{\boldsymbol{V}}, \qquad T' = T - \bar{T} \tag{21}$$

Let us assume that periodic conditions are reached:

$$\frac{\partial \bar{\boldsymbol{V}}}{\partial t} = 0, \qquad \frac{\partial \bar{T}}{\partial t} = 0 \tag{22}$$

At these conditions, in terms of the following quantities

$$\boldsymbol{F}_{V1} = \frac{\partial \boldsymbol{V}'}{\partial t}, \qquad \boldsymbol{F}_{V2} = \nabla \bar{p}, \qquad \boldsymbol{F}_{V3} = \nabla p'$$

$$\boldsymbol{F}_{V4} = \nabla\cdot[\bar{\boldsymbol{V}}\bar{\boldsymbol{V}}], \qquad \boldsymbol{F}_{V5} = \nabla\cdot[\bar{\boldsymbol{V}}\boldsymbol{V}'], \qquad \boldsymbol{F}_{V6} = \nabla\cdot[\boldsymbol{V}'\bar{\boldsymbol{V}}]$$

$$\boldsymbol{F}_{V7} = \nabla\cdot[\boldsymbol{V}'\boldsymbol{V}'], \qquad \boldsymbol{F}_{V8} = -Pr\nabla^2\bar{\boldsymbol{V}}, \qquad \boldsymbol{F}_{V9} = -Pr\nabla^2\boldsymbol{V}'$$

$$\boldsymbol{F}_{V10} = \frac{\Lambda\Omega^2}{Pr}\sin(\Omega t)\bar{T}\boldsymbol{n}, \qquad \boldsymbol{F}_{V11} = \frac{\Lambda\Omega^2}{Pr}T'\sin(\Omega t)\boldsymbol{n} \tag{23a}$$

$$F_{T1} = \frac{\partial T'}{\partial t}, \qquad F_{T2} = \nabla\cdot[\bar{\boldsymbol{V}}\bar{T}], \qquad F_{T3} = \nabla\cdot[\bar{\boldsymbol{V}}T']$$

$$F_{T4} = \nabla\cdot[\boldsymbol{V}'\bar{T}], \qquad F_{T5} = \nabla\cdot[\boldsymbol{V}'T'], \qquad F_{T6} = -\nabla^2 T$$

$$F_{T7} = -\nabla^2 T' \tag{23b}$$

Eqs. (19b) and (19c) read

$$\sum_{i=1}^{11} \boldsymbol{F}_{Vi} = 0 \tag{24a}$$

$$\sum_{i=1}^{7} F_{Ti} = 0 \tag{24b}$$

In the preceding equations, the generic term F_i present in Eqs. (19) can be considered the sum of an average value $\bar{F}_i(x, y)$ plus a periodic oscillation $F_i'(x, y)$:

$$\bar{F}_i(x, y) = \frac{\omega}{2\pi}\int_0^{2\pi/\omega} F_i(x, y)\,\mathrm{d}t, \qquad F_i' = F_i - \bar{F}_i \tag{25}$$

By definition, $\overline{F_i'} = 0$ so that for $i = 1, 3, 5, 6, 9$, and 10

$$\overline{\boldsymbol{F}_{vi}} = \boldsymbol{0} \tag{26a}$$

for $i = 1, 3, 4$, and 7

$$\overline{F_{Ti}} = 0$$

for $i = 2, 4$, and 8

$$\boldsymbol{F}_{vi}' = \boldsymbol{0} \tag{26b}$$

and for $i = 2$ and 6

$$F_{Ti}' = 0$$

Only the nonlinear periodic oscillating terms, appearing in Eqs. (24), that contain the product of oscillating quantities F_{v7}, F_{v11}, and F_{T5} have nonzero values of the time average

$$\boldsymbol{F}_{V7} = \bar{\boldsymbol{F}}_{V7} + \boldsymbol{F}'_{V7}, \qquad \boldsymbol{F}_{V11} = \bar{\boldsymbol{F}}_{V11} + \boldsymbol{F}'_{V11}$$

$$F_{T5} = \bar{F}_{T5} + F'_{T5} \tag{26c}$$

When averaging Eqs. (24a) and (24b), one gets

$$\sum_{i=1}^{11} \overline{\boldsymbol{F}_{Vi}} = 0 \tag{27a}$$

$$\sum_{i=1}^{7} \overline{F_{Ti}} = 0 \tag{27b}$$

then taking into account Eqs. (26a) and (26b), the set for the average balance equations reads

$$\nabla\cdot\bar{\boldsymbol{V}} = 0 \tag{28a}$$

$$(\nabla\bar{p}) + \nabla\cdot[\bar{\boldsymbol{V}}\bar{\boldsymbol{V}}] + \nabla\cdot[\overline{\boldsymbol{V}'\boldsymbol{V}'}]$$

$$= Pr(\nabla^2\bar{\boldsymbol{V}}) - \Lambda\Omega^2/Pr\,\overline{T'\sin(\Omega t)}\boldsymbol{n} \tag{28b}$$

$$\nabla\cdot[\bar{\boldsymbol{V}}\bar{T}] + \nabla\cdot[\overline{\boldsymbol{V}'T'}] + = \nabla^2\bar{T} \tag{28c}$$

Before going into details of the analysis, note the novelty and the merits of our proposed analysis. The fact that Eqs. (19) show terms containing average and/or oscillating variables allows us to perform a more detailed and accurate OMA. Let us take, for example, the energy equation (19c). A classical approach for the OMA is to estimate (without solving the equations) the order of magnitude of $\boldsymbol{V}$, T, and the length scales from which the order of magnitude of each term in the equation can be evaluated.

If we carry on the OMA before separating the average and the oscillating terms, then we are forced either to keep or to neglect terms treating both the oscillatory and the time-average components in the same way. On the other hand, once one identifies all of the terms, one must find a way to estimate both the amplitude of the oscillation and the average values of each variable and then to perform a selective analysis that leads to the identification of negligible terms. What is done in this paper is a sort of inverse OMA insofar as we have computed the weight of each term after solving the full set of equations. In this way, one gets a clear picture of the possibility of neglecting a number of terms instead of others (at different conditions) that very often lead to wrong conclusions, as will be discussed later.

The main goal of the present work is, therefore, to find the conditions at which some of the terms in Eqs. (19) and (28) can be neglected. Thus, one must, first, define a procedure for the evaluation, from the numerical solution, of the order of magnitude of each term of the equations at each field point and, then, to average properly over the entire flowfield. The terms $\overline{F_{vi}}$, F'_{vi}, $\overline{F_{Ti}}$, and F'_{Ti} are computed through the correct solution of the full Navier–Stokes equations by evaluating each term at each grid point during the period $2\pi/\omega$. As mentioned before, the analysis is made once periodic conditions are established. The order of magnitude of the zero-average terms is evaluated by computing the maximum $F_{i\max}$ and the minimum $F_{i\min}$ during the period $2\pi/\omega$:

$$\nabla F_i(x, y) = [F_i(x, y)]_{\max} - [F_i(x, y)]_{\min} \tag{29}$$

that represents the amplitude of the oscillatory part of the disturbance $F_i' = \Delta F_i\, f_i(t)/2$, where $f_i(t)$ is a periodic, zero time-average function, for example, $f_i(t) = \sin(\omega t + \varphi_i)$.

The numerical computation is performed over the N grid points, $j = 1, N$, and overall quantities are defined as

$$(F_i)_{ov} = \frac{1}{N}\sum_{j=1}^{N} |(F_i)_j| \tag{30}$$

in particular for the average and oscillatory terms,

$$(\bar{F}_i)_{ov} = \frac{1}{N}\sum_{j=1}^{N} |(\bar{F}_i)_j| \tag{31a}$$

$$(\Delta F_i)_{ov} = \frac{1}{N}\sum_{j=1}^{N} |(\Delta F_i)_j| \tag{31b}$$

Numerical Analysis of the ISS Microgravity Environment

We want to find different regimes and different simplified set of equations in the range of Λ and Ω (or vibrational Rayleigh number Ra_v) of practical interest for typical potential experimentation to be carried out on the ISS. The ISS is characterized by a complex microgravity environment with quasi-steady (residual) g (of the order of magnitude of microgravity) and a g-jitter spectrum $g(f)$ (Fig. 3). Themovibrational theory shows that, at high frequency (and small displacements ($\Omega \gg 1$ and $\Lambda \ll 1$), the steady-state disturbances increase with the vibrational Rayleigh number. Straight lines corresponding to three values of vibrational Rayleigh number Ra_v are in Fig. 3 that cover the range of $g(f)$ to be expected on the ISS and that are above and parallel to the so-called ISS requirement curve ($Ra_v \cong 3.3 \times 10^{-2}$). Moving along the lines $Ra_v = \text{const}$ at increasing frequency, one encounters different regimes corresponding to equations with different important terms. The parametric analysis was performed for $10 \le \Omega \le 10^5$ and $10^{-7} \le g_\omega/g_0 \le 10^{-2}$, which correspond to $3.3 \le Ra_v \le 3.3 \times 10^4$.

At large Ω, when the steady disturbances prevail over the oscillating ones (Fig. 2), one would expect that, according to the thermovibrational theory, the disturbances stay constant along the lines $Ra_v = \text{const}$. A lower limit of Ω for the validity of the thermovibrational theory (which has been shown to be correct for $\Omega \gg 1$) and the identification (in terms of Ω) of different regimes for which a simplified set of balance equations apply can be made by comparing the importance of the terms of the equations.

The numerical analysis has been made by solving the complete unsteady Navier–Stokes equations and by computing, a posteriori, each term of the momentum and energy equations for the amplitude of the periodic part and for the averaged ones. All of these terms have been plotted vs Ω in Figs. 4 and 5 for two values of Ra_v, 3.3×10^2 and 3.3×10^4, which correspond to maximum values to be expected on the ISS.

Comparison of the order of magnitude of each term of the equations is made by plotting the quantities Φ'_i and $\overline{\Phi_i}$ defined by the

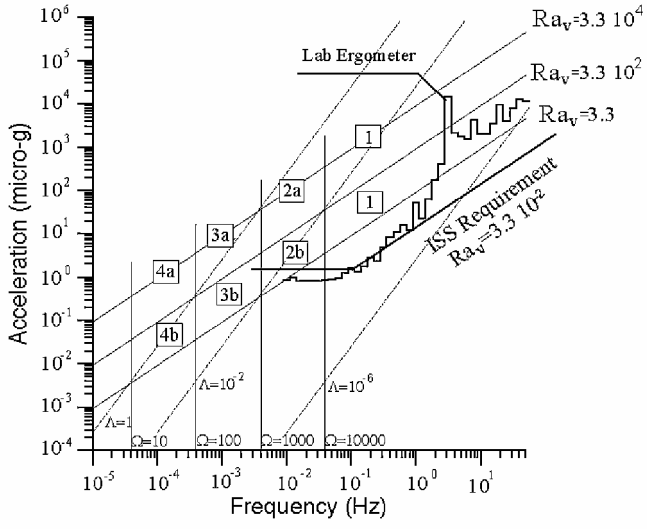

a)

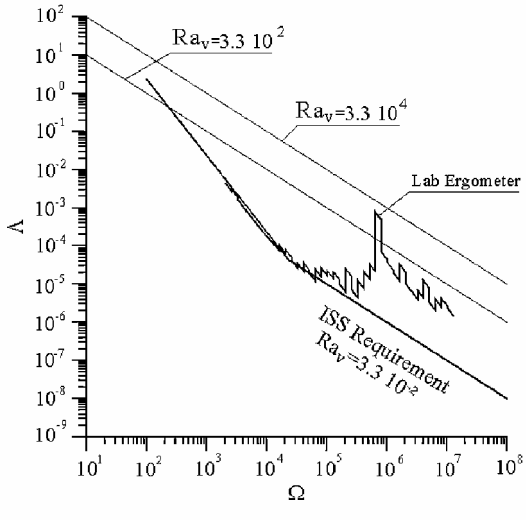

b)

Fig. 3 Comparison between predicted accelerations, ISS requirement curve, and lines of constant Λ, Ω, and vibrational Rayleigh number Ra_v in the a) acceleration frequency plane and b) Λ–Ω plane: $\Omega = \omega L^2/\alpha$, $\Lambda = b(\beta_T \Delta T/L)$, $Ra_v = (b\omega\beta_T \Delta TL)^2/2\nu\alpha$.

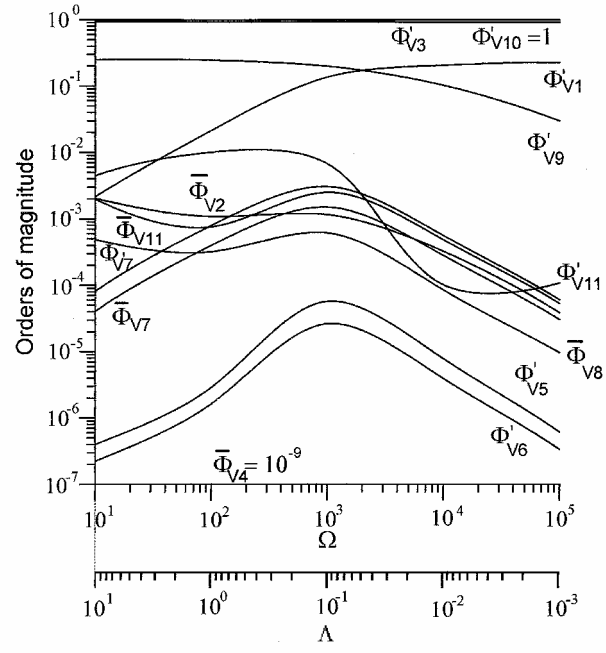

a)

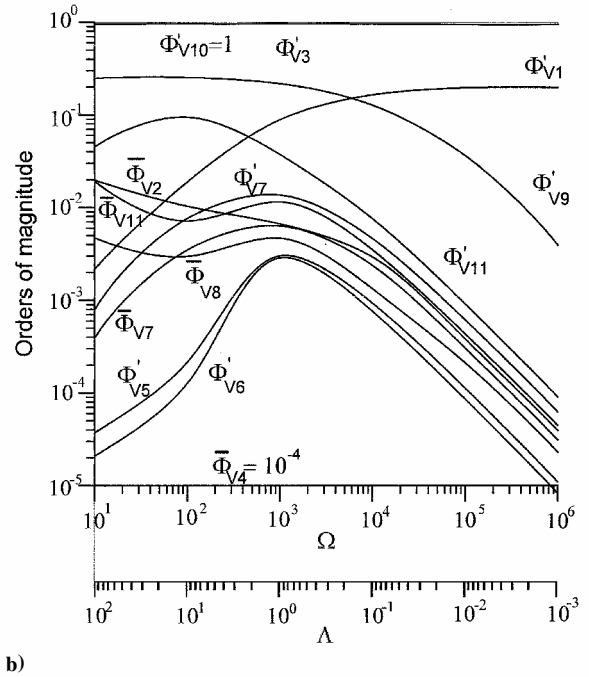

b)

Fig. 4 Comparison between the order of magnitude of the different terms involved in the momentum equation in the case Ra_v = a) 330 and b) 33,000: $\Omega = \omega L^2/\alpha$, $\Lambda = b(\beta_T \Delta T/L)$, and $Ra_v = \Omega^2\Lambda^2/2Pr$.

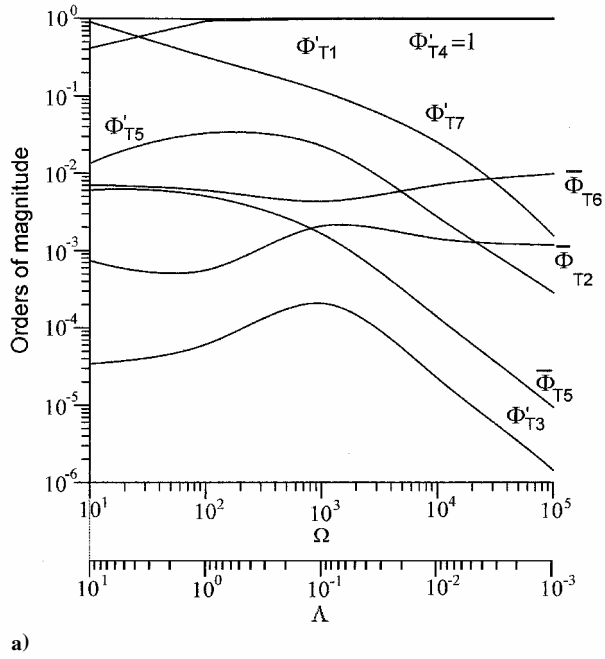

a)

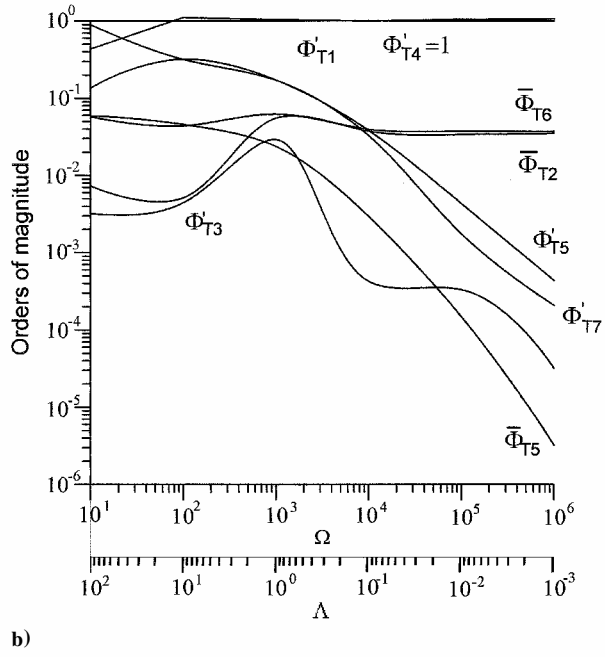

b)

Fig. 5 Comparison between the order of magnitude of the different terms involved in the energy equation in the case Ra_v = a) 330 and b) 33,000: $\Omega = \omega L^2/\alpha$, $\Lambda = b(\beta_T \Delta T/L)$, and $Ra_v = \Omega^2\Lambda^2/2Pr$.

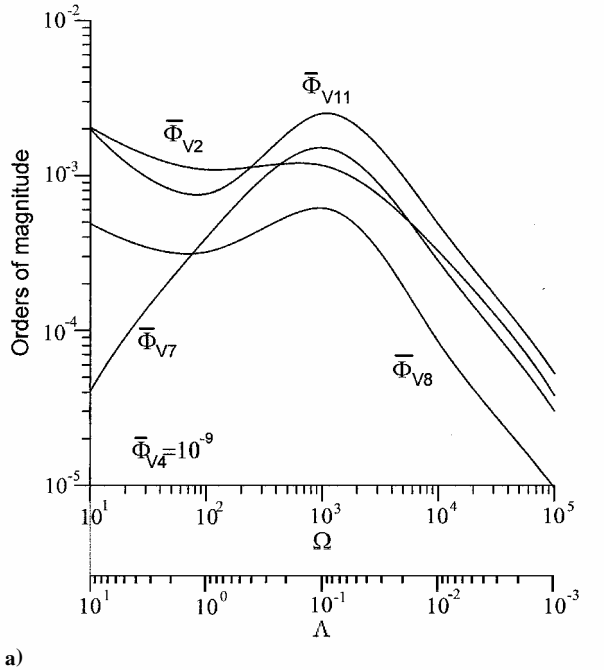

a)

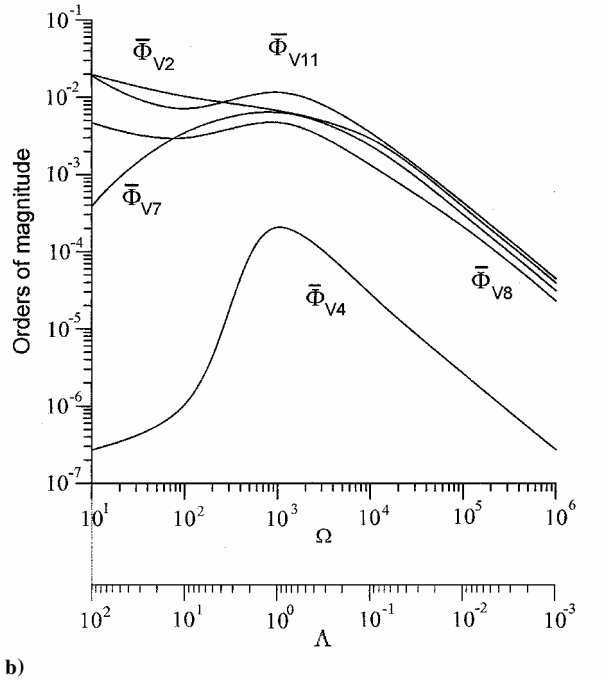

b)

Fig. 6 Comparison between the order of magnitude of the different terms involved in the averaged momentum equation in the case Ra_v = a) 330 and b) 33,000: $\Omega = \omega L^2/\alpha$, $\Lambda = b(\beta_T \Delta T/L)$, and $Ra_v = \Omega^2\Lambda^2/2Pr$.

ratios between each term i and the leading term in the momentum (subscript v) and energy (subscript T) equations. In particular,

$$\overline{\Phi_{vi}} = (\overline{F_{vi}})_{ov}/(\Delta F_{v10})_{ov}, \qquad \Phi'_{vi} = (\Delta F_{vi})_{ov}/(\Delta F_{v10})_{ov} \quad (32a)$$

$$\overline{\Phi_{Ti}} = (\overline{F_{Ti}})_{ov}/(\Delta F_{T4})_{ov}, \qquad \Phi'_{Ti} = (\Delta F_{Ti})_{ov}/(\Delta F_{T4})_{ov} \quad (32b)$$

where $(\Delta F_{v10})_{ov}$ is the driving term $g_\omega \beta_T(\bar{T} - T_0)$ and $(\Delta F_{T4})_{ov}$ corresponds to the convective energy transport $\nabla \cdot [\boldsymbol{V}'\bar{T}]$.

Analysis of Figs. 4 and 5 shows that the overall relative importance of each term depends on Ω and to a less extent on vibrational Rayleigh number Ra_v. For instance, at very high values of Ω only three terms in the momentum equation, Φ'_{v1}, Φ'_{v3}, and Φ'_{v10}, and two terms in the energy equation, Φ'_{T1} and Φ'_{T2} (thermovibrational theory), prevail (regime 1).

The terms appearing in the averaged momentum and energy equations are shown in Figs. 6 and 7. As a result of the comparison of the different terms, different regimes have been identified. In the Appendix the sets of equations for the different regimes for the full and averaged momentum and energy equations are indicated. Separation of the terms into those containing steady and oscillatory contributions shows that in the entire range of Ω and Λ (or Ω and vibrational Rayleigh number Ra_v) the leading terms in the complete momentum equation is the driving action $\boldsymbol{F}'_{v10} = (\Lambda\Omega^2/Pr)\bar{T}\sin\Omega t\boldsymbol{n}$, which is almost balanced by the pressure term $\boldsymbol{F}'_{v3} = \nabla p'$. At relatively low frequency, the other term to be taken into account is $\boldsymbol{F}'_{v9} = -Pr\nabla^2\boldsymbol{V}'$, which at $\Omega > 10^4$ can be neglected with respect to the term $\boldsymbol{F}'_{v1} = \partial\boldsymbol{V}'/\partial t$. In the energy transport equation, the two leading terms are $F'_{T1} = \partial T'/\partial t$ and $F'_{T4} = \nabla \cdot (\boldsymbol{V}'T)$. Unless at very low frequency ($\Omega < 10^2$), a third term must also be taken into account, $F'_{T7} = -\nabla^2 T'$. Therefore, the full and averaged equations can be summarized as follows.

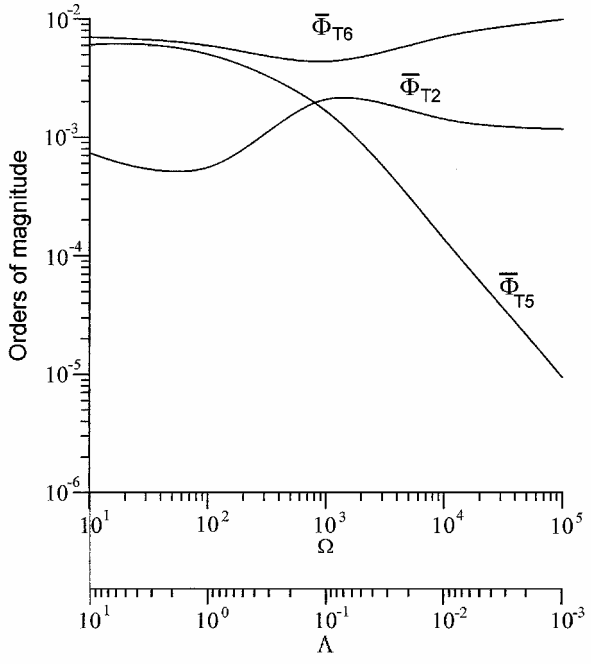

a)

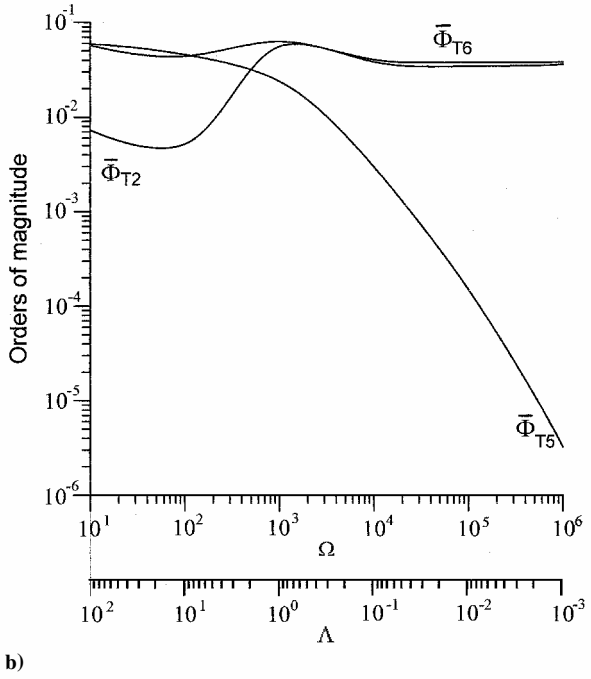

b)

Fig. 7 Comparison between the order of magnitude of the different terms involved in the averaged energy equation in the case Ra_v = a) 330 and b) 33,000: $\Omega = \omega L^2/\alpha$, $\Lambda = b(\beta_T \Delta T/L)$, and $Ra_v = \Omega^2\Lambda^2/2Pr$.

Full equations:

$$\frac{\Lambda\Omega^2}{Pr}\sin(\Omega t)\bar{T}\boldsymbol{n} + \nabla p' \begin{cases} = -Pr\nabla^2 \boldsymbol{V}' & \text{for} \quad \Omega < 10^3 \\ = \dfrac{\partial \boldsymbol{V}'}{\partial t} & \text{for} \quad \Omega > 10^3 \end{cases} \tag{33a}$$

$$\frac{\partial T'}{\partial t} + \nabla \cdot [\boldsymbol{V}'\bar{T}] \begin{cases} = \nabla^2 T' & \text{for} \quad \Omega < 10^2 \\ = 0 & \text{for} \quad \Omega > 10^3 \end{cases} \tag{33b}$$

Averaged equations:

$$\frac{\Lambda\Omega^2}{Pr}\overline{\sin(\Omega t)T'}\boldsymbol{n} + \nabla \bar{p} - Pr\nabla^2 \bar{\boldsymbol{V}} \begin{cases} = 0 & \text{for} \quad \Omega < 10^2 \\ = \nabla \cdot (\overline{\boldsymbol{V}'\boldsymbol{V}'}) & \text{for} \quad \Omega > 10^2 \end{cases} \tag{34a}$$

$$\nabla^2 \bar{T} \begin{cases} = \nabla \cdot [\bar{\boldsymbol{V}}\bar{T}] & \text{for} \quad \Omega > 10^3 \\ = \nabla \cdot [\overline{\boldsymbol{V}'T'}] & \text{for} \quad \Omega < 10^3 \end{cases} \tag{34b}$$

The simplest regime is that corresponding to $\Omega \gg 1$ and $\Lambda \ll 1$ (thermovibrational theory) for which approximate relations can be found for $\boldsymbol{V}'$ and T' as functions of the steady values ($\bar{\boldsymbol{V}}$, $\bar{T}$) and substituted in the averaged momentum equation, where the driving term and the term $\nabla \cdot (\overline{\boldsymbol{V}'\boldsymbol{V}'})$ (which has the same meaning of the turbulence Reynolds stresses) are put together, due to the same dependence on Λ and Ω. [See terms $(\overline{\Phi_{v11}})$ and $(\overline{\Phi_{v7}})$ in Fig. 6 for $\Omega > 10^3$.] Intermediate regimes with simplified equations (full and averaged) are indicated in Figs. 3 and in the Appendix.

OMA can be performed in the limiting cases of very low (quasi steady) or very high frequency. In this last case, the analysis yields orders of magnitudes of the disturbances, for example, thermal disturbances, which depend on the assumptions made on the negligibility of some terms in the momentum and energy equations (in particular, the nonlinear terms related to the forcing action and to the convective terms in the two equations). If all of these terms are ignored, the disturbance in the system consists of $\boldsymbol{V}'$ and T' without average disturbances. When the conditions are such that the nonlinear terms in the momentum equation are accounted for, that is, the thermovibrational conditions $\Omega \gg 1$ and $\Lambda \ll 1$ prevail, then the viscous term can be neglected, and the main effect of the driving term (with nonzero time average) is to generate a streaming or a steady average velocity field that is overimposed to an oscillating velocity field.

Even though all of the average terms appearing in the complete equations are of smaller order of magnitude and may appear negligible with respect to the periodic oscillating terms, one must consider that the streaming steady convective energy transport alters the temperature diffusive distribution more than the oscillating (zero time average) convection.

Indeed, it has been shown[12] that at different conditions very small steady residual-g (of the order of few micro-g) generate disturbance effects much larger than the high amplitude g-jitter (because their effects somehow average out over the forcing period).

Evaluation of Thermal Disturbances

The two nondimensional disturbances ($\bar{\varepsilon}_T$ and ε'_T) introduced earlier have been evaluated for two values of the vibrational Rayleigh numbers (330 and 33,330). After reaching the periodic conditions ($\partial\bar{\boldsymbol{V}}/\partial t = \boldsymbol{0}$ and $\partial\bar{T}/\partial t = 0$) time averages of $\boldsymbol{V}$ ($\bar{\boldsymbol{V}}$) and T ($\bar{T}$) are computed by means of the definitions (20).

The value of the difference with the diffusive solution and the temperature oscillation amplitudes are computed at each grid point j by the evaluation, in a period, of the average $\bar{T}$ and the difference between the maximum and the minimum. In terms of the nondimensional quantities and of the boundary conditions, $T_{dj} = x_j$, the temperature disturbances at each grid point j read

$$\overline{T_j} - T_{dj} = \overline{T_j} - x_j \tag{35}$$

$$\Delta T_j = [(T_j)_{\max} - (T_j)_{\min}]/2 \tag{36}$$

from which the two disturbance factors are defined (Figs. 2):

$$\overline{\varepsilon_T} = \frac{1}{N}\sum_{j=1}^{N}(\overline{T_j} - x_j)^2, \qquad \varepsilon'_T = \frac{1}{N}\sum_{j=1}^{N}\Delta T_j \tag{37}$$

Examination of Fig. 2b shows one of the main results of this study: As the curve $Ra_v = (\Lambda^2\Omega^2)/(2Pr) = \text{const}$, is followed, that is, moved along what is assumed today to be the ISS requirement, or the tolerable values of the amplitude of the acceleration vs the acceleration frequency, the value of $\bar{\varepsilon}_T$ tends to level out above, for example, $\Omega = 10^3$ (which for the considered reference case, corresponds to about 4×10^{-3} Hz; Fig. 3). The oscillating disturbance ε'_T rapidly decreases with increasing Ω, for instance, at a frequency $f = 4 \times 10^{-2}$ Hz ($\Omega = 10^4$) the value of ε'_T is almost two orders of magnitude lower. [At $f = 4$ Hz ($\Omega = 10^6$) ε'_T is five orders of magnitude lower.] Figure 2b refers to the case $Ra_v = 33{,}000$. Similar plots are obtained at different vibrational Rayleigh number Ra_v

with values of the maximum disturbances somehow proportional to vibrational Rayleigh number Ra_v.

The way the plots of $\bar{\varepsilon}_T$ and ε'_T are constructed (averaging over the period $2\pi/\omega$ and over the whole flowfield) suggests that these values can only give an order of magnitude of the overall disturbance; one cannot exclude the possibility that there might be some spots with disturbances higher than the computed ε_T and other points of the field where these disturbances are smaller, if not zero, for example, at the walls held at constant temperatures. The averaging in time and space, however, is likely to yield overall orders of magnitude that are less dependent on the specific geometry and on the boundary conditions.

A completely different issue is the evaluation of the disturbance effect on different microgravity processes of $\bar{\varepsilon}_T$ and ε'_T. Indeed, these two factors are not comparable, for instance, even when $\varepsilon'_T \ll \bar{\varepsilon}_T$ for experiments that exhibit a high sensitivity to unsteady conditions, one may not be in a position to neglect the first type of disturbance with respect to the second one .

The most critical conditions could occur at intermediate Ω, where both $\bar{\varepsilon}_T$ and ε'_T are of the same order (albeit less than their maxima). If one follows the ISS requirement curve ($g_\omega = 1\mu g$ for $\Omega < 10^3$ and $g_\omega \propto \Omega$ for $\Omega > 10^3$), one should expect that indeed in the low-frequency part ($Ra_v \propto \Omega^{-2}$) the value of $\varepsilon'_T \cong$ const (with negligible $\bar{\varepsilon}_T$), and in the high-frequency part ($Ra_v \cong$ const), then $\bar{\varepsilon}_T \cong$ const (with negligible ε'_T).

Figures 3a and 3b seem to show that the limit transition between $g =$ const to $g \cong \omega$ for ISS specification should be placed at $\Omega \cong 10^3$. Previous works on the tolerability limits (which in the present work correspond to limit values of ε'_T and $\bar{\varepsilon}_T$) apparently show some discrepancies that can be explained on the basis of the preceding analysis.

In Ref. 1 the assumption of the negligibility of the nonlinear convective terms with respect to the diffusive terms in both the momentum and energy equations at the high frequencies correctly led to oscillatory disturbance amplitudes in temperature, ε'_T, proportional to g/ω^2 but could not predict steady temperature disturbances. Similarly Naumann[15] neglected the nonlinear convective term $\bar{F}_{V7}$ in the study of the flow in an infinitely long two-dimensional cavity filled with a fluid subjected to an initial linear temperature distribution.

The present analysis shows that this assumption is not justified in the entire range of frequency and amplitude. [For $\Omega > 10^3$ and $\Lambda < 0.1$, the term $\bar{F}_{V7}$ in the average momentum equation is of the same order of magnitude of the leading terms (Fig. 6)]. As a result of the assumptions made, Naumann[15] found a concentration (or thermal) average disturbance $\bar{\varepsilon}_C$ (or $\bar{\varepsilon}_T$) proportional to g^2/Ω^4, whereas the present analysis shows that $\bar{\varepsilon}_T$ is proportional to g^2/Ω^2, although Naumann refers to study cases with different aspect ratios.

Conclusions

The difference and the meaning of the two disturbance parameters $\bar{\varepsilon}$ and ε' with respect to the diffusive distributions of scalar quantities (energy and species) have been clarified. The relative importance of the two contributions depends in a different manner on the frequency of the acceleration and (to a less extent) its amplitude. Previous results available in literature, which seemed to be contradictory, are explained by recognizing that some of them refer to ε' and others to $\bar{\varepsilon}$. It is shown that, at low frequencies, the main contributions are given by ε' (which for $\Omega \ll 1$ refers to quasi-steady regimes); at relatively high frequencies ($\Omega \gg 1$), $\bar{\varepsilon} \gg \varepsilon'$ as predicted by the thermovibrational theory. The possibility of evaluating the order of magnitude and the trends of $\bar{\varepsilon}$ and ε' at high Ω has been confirmed for the study case. In the intermediate frequency regimes ($\Omega \cong 10^3$), both $\bar{\varepsilon}$ and ε' have same order of magnitude.

In these regimes, one may neglect different terms in the equations; the analysis made suggests different sets of equations obtained by the omission of some terms; the terms that could be omitted have been identified by a detailed analysis made by separating the average from the oscillating part. The risk of omitting nonnegligible terms may lead to wrong conclusions.

The set of simplified equations, in the related ranges of validity, can be used to develop analytical and/or mixed numerical/analytical methods that can significantly speed up the simulation of the phenomena under investigation, with respect to the solution of the complete Navier–Stokes equations.

Appendix: Equations of the Different Regimes

The numerical simulation performed for $\Omega > 10{,}000$ (regime 1) and $Ra_v = 10^5/3$ shows that the simplified set of equation corresponds to the Gershuni and Lyubimov[14] equations. ($\bar{\Phi}_{V4}$ and $\bar{\Phi}_{T5}$ are negligible in the momentum and in the energy-averaged equations, respectively. In the complete equations only the terms Φ'_{V1}, Φ'_{V3}, Φ'_{V10}, Φ'_{T1}, and Φ'_{T4}, are relevant.

Regime 1

The complete equations are

$$\frac{\partial \boldsymbol{V}'}{\partial t} + \frac{1}{\rho_0}\nabla p' = b\omega^2\beta_T(\bar{T} - T_0)\sin(\omega t)\boldsymbol{n} \tag{A1a}$$

$$\frac{\partial T'}{\partial t} + \nabla\cdot[\boldsymbol{V}'\bar{T}] = 0 \tag{A1b}$$

The averaged equations are

$$\frac{1}{\rho_0}\nabla\bar{p} + \overline{\boldsymbol{\nabla}\cdot[\boldsymbol{V}'\boldsymbol{V}']} = \nu\nabla^2\bar{\boldsymbol{V}} + b\omega^2\beta_T\overline{T'\sin(\omega t)}\boldsymbol{n} \tag{A1c}$$

$$\nabla\cdot[\bar{\boldsymbol{V}}\bar{T}] = \alpha\nabla^2\bar{T} \tag{A1d}$$

For $1000 < \Omega < 10{,}000$ (regime 2a) other terms appear in the instantaneous time-dependent flow quantities with respect to the Gershuni and Lyubimov[14] formulation; the terms Φ'_{V9}, Φ'_{T5}, and Φ'_{T7} are no longer negligible in the momentum and energy equations, respectively. Moreover, the term $\bar{\Phi}_{T5}$ appears in the averaged-energy equation.

Regime 2a

The complete equations are

$$\frac{\partial \boldsymbol{V}'}{\partial t} + \frac{1}{\rho_0}\nabla p' = b\omega^2\beta_T(\bar{T} - T_0)\sin(\omega t)\underline{n} + \nu\nabla^2 V' \tag{A2a}$$

$$\frac{\partial T'}{\partial t} + \nabla\cdot[\boldsymbol{V}'\bar{T}] + \nabla\cdot[\boldsymbol{V}'T'] = \alpha\nabla^2 T' \tag{A2b}$$

The averaged equations are

$$(1/\rho_0)\nabla\bar{p} + \overline{\nabla\cdot[\boldsymbol{V}'\boldsymbol{V}']} = \nu\nabla^2\bar{\boldsymbol{V}} + b\omega^2\beta_T\overline{T'\sin(\omega t)}\boldsymbol{n} \tag{A2c}$$

$$\nabla\cdot[\bar{\boldsymbol{V}}\bar{T}] + \overline{\nabla\cdot[\boldsymbol{V}'T']} = \alpha\nabla^2\bar{T} \tag{A2d}$$

For $100 < \Omega < 1000$ (regime 3a), with respect to regime 2a, the terms Φ'_{V1} and $\bar{\Phi}_{T2}$ become negligible, whereas the term Φ'_{V11} appears.

Regime 3a

The complete equations are

$$\frac{1}{\rho_0}\nabla p' = b\omega^2\beta_T(\bar{T} - T_0)\sin(\omega t)\boldsymbol{n} + b\omega^2\beta_T T'\sin(\omega t)\boldsymbol{n} + \nu\nabla^2\boldsymbol{V}' \tag{A3a}$$

$$\frac{\partial T'}{\partial t} + \nabla\cdot[\boldsymbol{V}'\bar{T}] + \nabla\cdot[\boldsymbol{V}'T'] = \alpha\nabla^2 T' \tag{A3b}$$

The averaged equations are

$$(1/\rho_0)\nabla\bar{p} + \overline{\nabla\cdot[\boldsymbol{V}'\boldsymbol{V}']} = \nu\nabla^2\bar{\boldsymbol{V}} + b\omega^2\beta_T\overline{T'\sin(\omega t)}\boldsymbol{n} \tag{A3c}$$

$$\overline{\nabla\cdot[\boldsymbol{V}'T']} = \alpha\nabla^2\bar{T} \tag{A3d}$$

For $10 < \Omega < 100$ (regime 4a) , with respect to regime 3a, the terms Φ'_{T1}, Φ'_{T5}, and $\bar{\Phi}_{V7}$ become negligible.

Regime 4a

The complete equations are

$$(1/\rho_0)\nabla p' = b\omega^2\beta_T(\bar{T} - T_0)\sin(\omega t)\boldsymbol{n} + b\omega^2\beta_T T'\sin(\omega t)\boldsymbol{n} + \nu\nabla^2\boldsymbol{V}' \quad \text{(A4a)}$$

$$\nabla\cdot[\boldsymbol{V}'\bar{T}] = \alpha\nabla^2 T' \quad \text{(A4b)}$$

The averaged equations are

$$(1/\rho_0)\nabla\bar{p} = \nu\nabla^2\bar{\boldsymbol{V}} + b\omega^2\beta_T\overline{T'\sin(\omega t)}\boldsymbol{n} \quad \text{(A4c)}$$

$$\overline{\nabla\cdot[\boldsymbol{V}'T']} = \alpha\nabla^2\bar{T} \quad \text{(A4d)}$$

Hereafter the regimes corresponding to $Ra_v = 10^3/3$ are denoted as the b regimes: For $\Omega > 10{,}000$ (regime 1b), the simplified set of equation corresponds to the Gershuni equations as for $Ra_v = 10^5/3$. For $1000 < \Omega < 10{,}000$ (regime 2b), with respect to the regime 2a, the term Φ'_{T5} becomes negligible.

Regime 2b

The complete equations are

$$\frac{\partial\boldsymbol{V}'}{\partial t} + \frac{1}{\rho_0}\nabla p' = b\omega^2\beta_T(\bar{T} - T_0)\sin(\omega t)\boldsymbol{n} + \nu\nabla^2\boldsymbol{V}' \quad \text{(A5a)}$$

$$\frac{\partial T'}{\partial t} + \nabla\cdot[\boldsymbol{V}'\bar{T}] = \alpha\nabla^2 T' \quad \text{(A5b)}$$

The averaged equations are

$$(1/\rho_0)\nabla\bar{p} + \overline{\nabla\cdot[\boldsymbol{V}'\boldsymbol{V}']} = \nu\nabla^2\underline{\bar{\boldsymbol{V}}} + b\omega^2\beta_T\overline{T'\sin(\omega t)}\boldsymbol{n} \quad \text{(A5c)}$$

$$\nabla\cdot[\bar{\boldsymbol{V}}\bar{T}] + \overline{\nabla\cdot[\boldsymbol{V}'T']} = \alpha\nabla^2\bar{T} \quad \text{(A5d)}$$

For $100 < \Omega < 1000$ (regime 3b), with respect to regime 3a, the term Φ'_{V11} disappears.

Regime 3b

The complete equations are

$$\frac{1}{\rho_0}\nabla p' = b\omega^2\beta_T(\bar{T} - T_0)\sin(\omega t)\boldsymbol{n} + \nu\nabla^2\boldsymbol{V}' \quad \text{(A6a)}$$

$$\frac{\partial T'}{\partial t} + \nabla\cdot[\boldsymbol{V}'\bar{T}] + \nabla\cdot[\boldsymbol{V}'T'] = \alpha\nabla^2 T' \quad \text{(A6b)}$$

The averaged equations are

$$(1/\rho_0)\nabla\bar{p} + \overline{\nabla\cdot[\boldsymbol{V}'\boldsymbol{V}']} = \nu\nabla^2\bar{\boldsymbol{V}} + b\omega^2\beta_T\overline{T'\sin(\omega t)\boldsymbol{n}} \quad \text{(A6c)}$$

$$\overline{\nabla\cdot[\boldsymbol{V}'T']} = \alpha\nabla^2\bar{T} \quad \text{(A6d)}$$

For $10 < \Omega < 100$ (regime 4b), with respect to regime 4a, the term Φ'_{V11} disappears.

Regime 4b

The complete equations are

$$(1/\rho_0)\nabla p' = b\omega^2\beta_T(\bar{T} - T_0)\sin(\omega t)\boldsymbol{n} + \nu\nabla^2\boldsymbol{V}' \quad \text{(A7a)}$$

$$\nabla\cdot[\boldsymbol{V}'\bar{T}] = \alpha\nabla^2 T' \quad \text{(A7b)}$$

The averaged equations are

$$(1/\rho_0)\nabla\bar{p} + \nu\nabla^2\bar{\boldsymbol{V}} + b\omega^2\beta_T\overline{T'\sin(\omega t)\boldsymbol{n}} \quad \text{(A7c)}$$

$$\overline{\nabla\cdot[\boldsymbol{V}'T']} = \alpha\nabla^2\bar{T} \quad \text{(A7d)}$$

Acknowledgments

This work has been partially supported by the Italian Space Agency. The authors thank R. Monti for many helpful discussions on the subject.

References

[1]Monti, R., Langbein, D. and Favier, J. J., "Influence of Residual Accelerations on Fluid Physics and Material Science Experiments," *Fluid and Material Science in Space*, edited by H. U. Walter, Springer-Verlag, Berlin, 1987.

[2]McFadden, G. B., and Coriell, S. R., "Solutal Convection During Directional Solidification," AIAA Paper 88-3635, July 1988.

[3]Schneider, S., and Straub, J., "Influence of the Prandtl number on Laminar Natural Convection in a Cylinder Caused by *g*-Jitter," *Journal of Crystal Growth*, Vol. 97, No. 1, 1989, pp. 235–242.

[4]Alexander, J. I. D., "Low Gravity Experiment Sensitivity to Residual Acceleration: A Review," *Microgravity Science and Technology*, Vol. 3, No. 1, 1990, pp. 52–68.

[5]Ramachandran, N., "G-Jitter Convection in Enclosures," 9th International Heat Transfer Conf., Paper 8-MC-03, Aug. 1990.

[6]Monti, R., and Savino, R., "The Basis and the Recent Developments of OMA and Its Applications to Microgravity," *Microgravity Quarterly*, Vol. 5, No. 1, 1994, pp. 13–17.

[7]Monti, R., and Savino, R., "A New Approach to *g*-Level Tolerability for Fluid and Material Science experiments," *Acta Astronautica*, Vol. 37, Oct. 1995, pp. 313–331.

[8]Monti, R., and Savino, R., "Influence of *g*-Jitter on Fluid Physics Experimentation On-board the International Space Station," *Space Station Utilisation Symposium*, ESA, SP-385, Dec. 1996, pp. 215–224.

[9]Monti, R., and Savino, R., "Microgravity Experiment Acceleration Tolerability on Space Orbiting Laboratories," *Journal of Spacecraft and Rockets*, Vol. 33, No. 5, 1996, pp. 707–716.

[10]Savino, R., and Monti, R., "Convection Induced by Residual-*g* and *g*-Jitters in Diffusion Experiments," *International Journal of Heat and Mass Transfer*, Vol. 42, No. 1, 1999, pp. 111–126.

[11]Savino, R., and Monti, R., "Improving Diffusion Controlled Microgravity Experiments by Facility Orientation," *Journal of Aerospace Engineering*, Vol. 212, Pt. G, 1998, pp. 415–426.

[12]Savino, R., and Monti, R., "Fluid Dynamic Experiment Sensitivity to Accelerations Prevailing on Microgravity Platforms," *Physics of Fluids in Microgravity*, Taylor and Francis, Philadelphia, 2001, pp. 515–559.

[13]Gershuni, G. Z., Zhukhovitskii, E. M., and Yurkov, Y. S., "Vibrational Thermal Convection in a Rectangular Cavity," *Izvestiya Akademii* Nauk SSSR, Mekh. Zhidk. Gaza, Vol. 4, No. 1, 1982, pp. 94–99.

[14]Gershuni, G. Z., and Lyubimov, D. V., *Thermal Vibrational Convection*, Wiley, New York, 1998, pp. 232–259.

[15]Naumann, R. J., "An Analytical Model for Transport from Quasi-Steady and Periodic Accelerations on Spacecraft," *International Journal of Heat and Mass Transfer*, Vol. 43, No. 16, 2000, pp. 2917–2930.

J. C. Taylor
Associate Editor